Journal of Alloys and Compounds 525 (2012) 166–171

Contents lists available at SciVerse ScienceDirect

Journal of Alloys and Compounds

journal homepage: www.elsevier.com/locate/jallcom

On the magnetic properties of pseudo-Laves phases $RE_{1-y}Y_yNi_{4-x}Al_xMg$ with RE = La, Ce and Gd prepared by both melting and ball milling

S. Couillaud[a], B. Chevalier[a], V. Paul-Boncour[b], J.-L. Bobet[a,*]

[a] CNRS, Université de Bordeaux, ICMCB, 87 Avenue du Docteur Albert Schweitzer, 33600 Pessac, France
[b] ICMPE-CMTR, CNRS-UPEC, UMR 7182, 2-8 rue Henri Dunant, 94320 Thiais, France

ARTICLE INFO

Article history:
Received 14 November 2011
Received in revised form 2 February 2012
Accepted 6 February 2012
Available online xxx

Keywords:
Magnetic properties
Structural properties

ABSTRACT

Magnetic properties of $RE_{1-y}Y_yNi_{4-x}Al_xMg$ (RE = La, Ce and Gd) are reported. $LaNi_4Mg$ displays a weak magnetization indicating that Ni is non magnetic as often observed in $RENi_2$ compounds. The magnetization of $CeNi_4Mg$ compounds shows a Curie Weiss behaviour with an effective paramagnetic moment $\mu_{eff} = 2.2\ \mu_B$. The magnetization of Gd compounds is dominated by the contribution of Gd moment with a paramagnetic effective moment close to $7.7\ \mu_B$/Gd for all studied compounds. The Curie temperature, which is 75 K for $GdNi_2$, decreases almost linearly with the number of Gd neighbours when more than half Gd is replaced by Y. The decrease of crystallinity of $GdNi_4Mg$, which is monitored by ball milling and heat treatment, strongly influences the magnetic properties and a relationship between the transition temperature and the crystallites size is reported.

1. Introduction

New ternary intermetallics based on magnesium have been widely studied during the past 10 years mainly because of their possible high hydrogen sorption properties. The rich Mg or RE ternaries (*e.g.* Gd_4TMMg, $La_2Mg_{17-x}TM_x$) (RE = Rare Earth, TM = transition metal) cannot offer any reversibility under normal conditions as they contain too many elements forming stable hydrides. For that reason, it is necessary to formulate a ternary composition richer in transition metal and with less RE and Mg. Moreover, some structure types ($CaCu_5$, $MgCu_2$) are well known to offer several interstitial sites for H atoms. For these reasons, we have been studying the $RENi_4Mg$ compounds. They crystallize in the F-43m space group (cubic $MgCu_4Sn$ structure type, known as C15b). This structure type can be considered as ordered ternary derivative of the $AuBe_5$ type structure (space group F-43m) in which Mg occupies the Au site (4*a*: 0 0 0) and Sn one of the Be sites (4*c*: 1/4 1/4 1/4). Known representatives containing both RE and Ni include a wide variety of RE (*e.g.* La, Ce, Nd, Gd and Y) [1,2].

Beside their hydrogenation properties, the magnetic properties of these $RENi_4Mg$ pseudo-Laves phases are also interesting to study. Magnetism of the Laves compounds $RETM_2$ have been an important subject since the ferromagnetism of $ZrZn_2$ found by Matthias and Bozorth in the mid to late 1950 [3]. In $RETM_2$ Laves phases, the magnetic properties result from the interaction between the localized magnetism of the RE and the itinerant magnetism of the 3d transition metal which could lead to a wide variety of magnetic structures [4,5]. Transition metals in RE–TM compounds and alloys exhibit gradually decreasing magnetic moments with increasing RE concentration and, in general, Ni in $RENi_2$ compounds is well known to loss its magnetic moment in the Laves phase compounds. This has been explained in terms of the outer shell electrons of the RE occupying the 3d band of the TM and is known as the charge-transfer model [6–10]. Through many extensive investigations, this model has been established and, at present, has become one of the most important clues to understand the magnetism of RE–TM intermetallics.

Most of the rare earth compounds $RENi_2$ order ferromagnetically at low temperatures due to the exchange interaction of the 4f magnetic moments through the conduction electrons (so called Ruddermann–Kittel–Kasuya–Yosida or RKKY interactions) [10]. The loss of the Ni magnetic moment in $GdNi_2$ compounds was subject of controversy because the Gd magnetic moment which is responsible for the magnetization varies from 7.0 to $7.2\ \mu_B$. An antiparallel coupling between Gd and Ni was evidenced by Yano et al. [11] with a moment of $0.24\ \mu_B$/Ni evaluated from the saturation magnetization at 4.2 K.

The structural and magnetic properties of $RE_{1-y}Y_yNi_{4-x}Al_xMg$ (RE = La, Ce and Gd) are reported here in complement to previous work [2,12,13]. Such pseudo-Laves phases can be of great interest as the Mg is replacing half of the RE in the structure, and can modify the RE–RE interactions. For example, Mg is acting as a dilution agent for the coupling of Gd magnetic moment. In order to increase the dilution, Y has also been used since a Gd-Y solid solution exists in

---

* Corresponding author.
E-mail address: bobet@icmcb-bordeaux.cnrs.fr (J.-L. Bobet).

0925-8388/$ – see front matter © 2012 Elsevier B.V. All rights reserved.
doi:10.1016/j.jallcom.2012.02.054

Table 1
Cell and magnetic parameters of $RE_{1-y}Y_yNi_{4-x}Al_xMg$ compounds.

Compound	a (Å)	T_C (K)	M_s (μ_B)	μ_{eff} (μ_B/Gd)	θ_P (K)
$LaNi_4Mg$	7.168(3)				
$CeNi_4Mg$	7.017(3)		0.38(1)	2.2	−53
$Ce_{0.5}Y_{0.5}Ni_4Mg$	7.006(3)		0.36 (1)		
$GdNi_4Mg$	7.041(2)	77(1)	4.6(1)	7.72	25.5
$Gd_{0.75}Y_{0.25}Ni_4Mg$	7.036(5)	62(1)	4.4(1)	7.68	6.9
$Gd_{0.5}Y_{0.5}Ni_4Mg$	7.029(6)	45(1)	2.7(1)	7.70	2.7
$Gd_{0.5}Y_{0.5}Ni_{3.5}Al_{0.5}Mg$	7.077(3)	15(1)	3.1(1)	7.75	5.2

the full range of composition and since both elements exhibit the same metallic radius (*i.e.* 1.801 Å for Y and 1.802 Å for Gd). Some Ni was also replaced by Al in order to get a better understanding of the RKKY interactions. Finally, as magnetic nanostructures often exhibit a different behaviour than bulk materials [14], ball milling was applied to the sample to get information about the influence of the microstructure on the magnetic properties.

2. Experimental

Compounds were prepared by melting the pure elements (STREM Chemicals, purity > 99.5%), placed in a tantalum crucible sealed under argon and melted at 1050 °C, followed by an annealing at 650 °C for 2 h. A slow cooling was applied to limit the Mg/RE exchange. Ball milling could also be applied after melting and subsequent heat treatment to obtain nanocrystalline materials.

The ball milled (BM) $GdNi_4Mg$ was prepared by mixing GdNi precursor and pure elemental powders of Mg and Ni (STREM Chemicals, purity > 99.5%) in an argon dry box with appropriate stoichiometry. The mix powder was put in a stainless steel container hermetically closed (weight ratio $m_{powders}/m_{balls} = 1{:}20$) and ball milled with a Fritsch P5 equipment with a plateau rotation speed of 250 rpm. The milling was performed for 10 h continuously and the samples were then collected under argon, cold pressed into pellets of about 1 g and finally annealed at 650 °C for 1 h in an evacuated sealed silica tube placed in an electric furnace.

The chemical composition (EPMA with a CAMECA SX-100) as well as the structural properties (X-ray powder diffraction with a Philips PW 1050 diffractometer) were checked prior any magnetic measurements to ensure the highest purity of the products.

Magnetization measurements were carried out using a MPMS-5S Quantum Design SQUID magnetometer and a PPMS09 from Quantum Design, using the ACMS option. Isofields magnetization curves were recorded between 4.2 and 300 K with applied fields of 0.1 T and 0.3 T. The measurements were generally performed with decreasing temperature. Isotherm magnetization curves were measured in the temperature range between 4.2 and 300 K with decreasing field from 9 T to −0.2 T.

The Differential Scanning Calorimetry (DSC) was performed with a Setaram Sensys Evo 600. Between 30 and 50 mg of sample were precisely weighted and introduced in a aluminium crucible of 100 μL. The sample was heated up to 500 °C under purified argon atmosphere and both heating and cooling rates were 5 K/min.

3. Results and discussion

All the samples presented in Sections 3.1–3.3 are prepared by melting and subsequent annealing to ensure the highest homogeneity of the compound. The lattice parameters and magnetic results are summarized in Table 1.

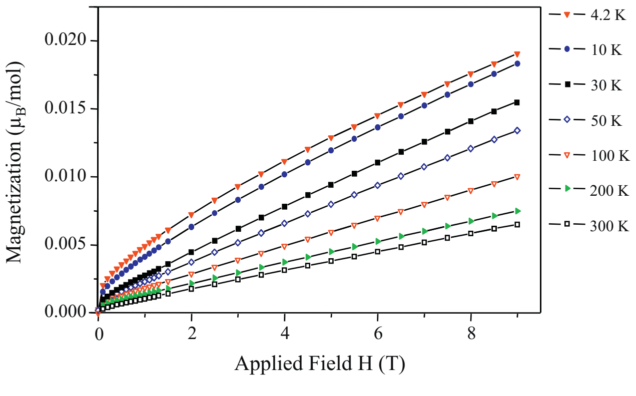

Fig. 1. $LaNi_4Mg$ magnetization as a function of applied fields at various temperatures.

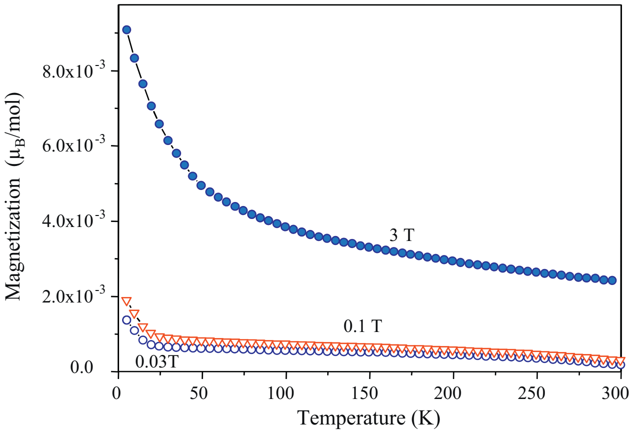

Fig. 2. $LaNi_4Mg$ magnetization as a function of temperature for various applied fields.

3.1. $LaNi_4Mg$ compound

The $LaNi_4Mg$ compound is single phase from the XRD point of view. However, the EPMA reveals the presence of some traces of elemental Ni. The XRD patterns were fully indexed within the F-43m space group (structure type $MgCu_4Sn$), $a = 7.168(3)$ Å for $LaNi_4Mg$.

The magnetizations were measured as a function of the applied field at various temperatures in the range from 4.2 to 300 K and are presented in Fig. 1. The magnetization remains very weak (<0.020 μ_B/mol) and even at very low temperature (*i.e.* 4.2 K) the saturation is not reached. Magnetizations as a function of temperature are shown in Fig. 2 and confirm the previous results. A small increase of the magnetization at low temperature can be consistent with a weak ferromagnetic contribution coming from an impurity which has not been detected by XRD either by EPMA.

Our results agree well with the fact that La is nonmagnetic (*i.e.* La^{3+} ion does not have any 4f electrons) and that Ni can have a small magnetic contribution in $RENi_2$ type compounds in agreement with previous works [11,15].

3.2. $Ce_{1-y}Y_yNi_4Mg$ compounds

As for the previous compounds, the Ce based compounds are single phase according to XRD (*e.g.* $a = 7.017(1)$ Å for $CeNi_4Mg$) but present some small impurities of binary Ce–Ni phase from the EPMA analysis. In Fig. 3, it appears that a ferromagnetic contribution exists even at room temperature (about 0.15 μ_B at 300 K under 9 T). This contribution can result from some ferromagnetic Ni particles, segregated at the surface of the compound. It also appears that even at low temperature the saturation is not completely reached

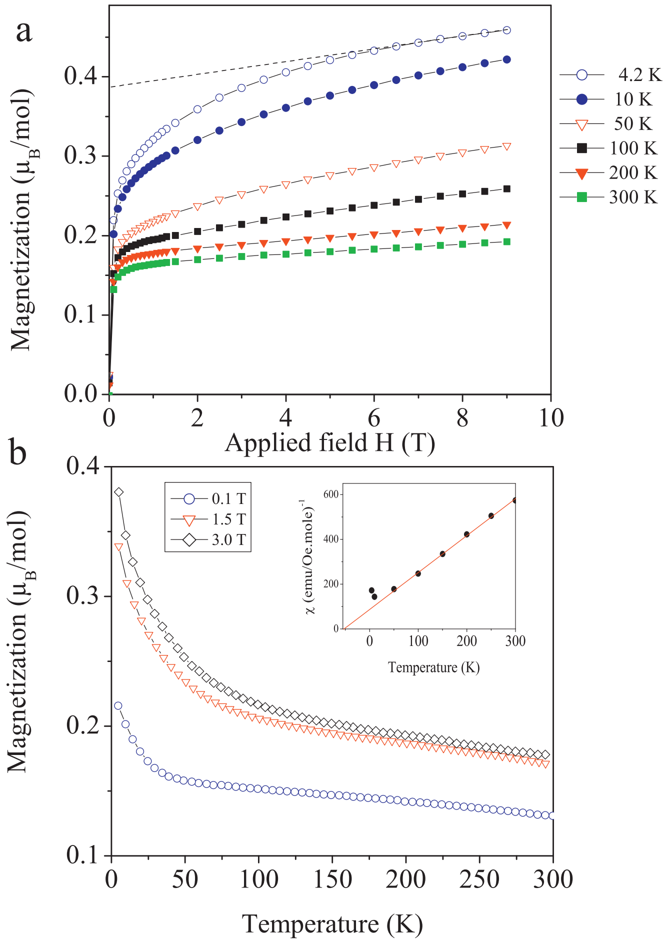

Fig. 3. (a) $CeNi_4Mg$ magnetization as a function of applied fields at various temperatures. (b) $CeNi_4Mg$ thermomagnetization at various applied fields. Inset is reverse susceptibility calculated with the slope of the *M*(*H*) curves.

for applied field up to 9 T. As seen in Fig. 3a, the saturation was therefore estimated from the tangent of the curve above 5 T and a value of 0.38 μ_B/mol was found. The inverse susceptibility (χ^{-1}) as a function of temperature, which has been deduced from the slope of the M(H) curves, exhibits a linear variation (Fig. 3b). Assuming that it corresponds to a Curie Weiss law, a paramagnetic effective moment of 2.2 μ_B can be calculated. This value is slightly lower than the one of free Ce^{3+} (*i.e.* 2.52 μ_B). Moreover the negative value of $\theta_P = -53$ K indicates that an antiferromagnetic coupling should exist in the compound. Therefore the assumption that Ni moment is not negligible (from Yano's work [11]) and that it is coupled antiparallel with the Ce moment can be assumed. Future works should be done to clarify this point. The $Ce_{0.5}Y_{0.5}Ni_4Mg$ compound exhibits a similar behaviour with a saturated magnetization of 0.37 μ_B at 4.2 K under 9 T.

Geibel et al. [16] have assumed that in $CeNi_4Mg$ the cerium was intermediate valent due to a smaller and less temperature dependent susceptibility than CePdMg. Nevertheless they show only χ for $CeNi_4Mg$ and $1/\chi$ for CePdMg which makes the comparison difficult. In Ref. [12], only $\chi(T)$ is reported, and the compound is described as a Pauli paramagnet. In [17] a more complete study of $CeNi_4Mg$ has been performed by neutron diffraction and Density of State (DOS) calculation. The Ce atoms are found to occupy only the 4*a* site and the Mg the 4*c* site (only 5% of mixing was refined). The DOS calculations show that Ce should be in an intermediate valent state.

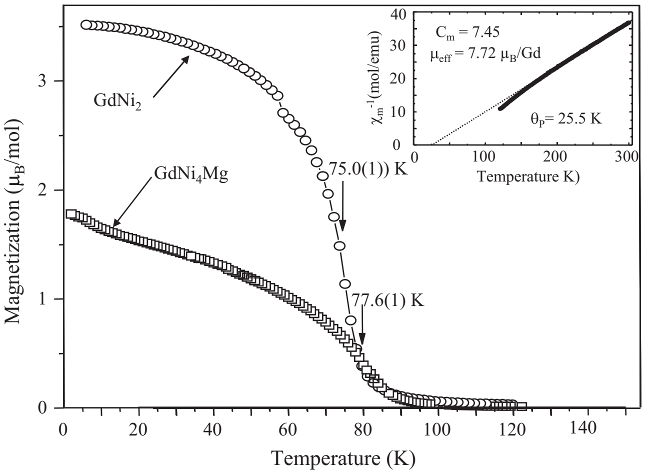

Fig. 4. $GdNi_4Mg$ (and $GdNi_2$ for comparison) magnetization as a function of temperature under an applied field of 0.1 T. Inset is the reverse susceptibility as a function of T for $GdNi_4Mg$ under 3 T.

In the present work, we did not observe a magnetic ordering of Ce at low temperature and therefore the Curie Weiss behaviour should be rather related to the nature of the Ce–Ni bonding than to the existence of trivalent cerium.

3.3. $Gd_{1-y}Y_yNi_{4-x}Al_xMg$ compounds

The thermomagnetization of $GdNi_4Mg$ (*i.e.* $Gd_{0.5}Mg_{0.5}Ni_2$) is compared with the $GdNi_2$ one in Fig. 4. In $GdNi_2$ compound a ferromagnetic transition occurs below a Curie temperature $T_C = 75$ K resulting from an indirect coupling between the Gd moments through the conducting electrons *via* a RKKY interactions [10]. Because of the weak radial density of the 4f electrons in rare earths, they cannot interact directly. The 5d electrons belonging to the outer shells of the RE transfer to the nickel, occupying the Ni 3d band [18]. As a result the 3d band is filled, the DOS at the Fermi level decreases and the Ni moment is reduced (0.24 μ_B/Ni in $GdNi_2$ estimated from the saturation magnetization at 4.2 K). Since Mg is diamagnetic the total magnetization of $GdNi_4Mg$ is dominated by the Gd moment contribution. Both $GdNi_2$ and $GdNi_4Mg$ present an increase of the magnetization at low temperature which is due to the ferromagnetic coupling between the Gd moments. $GdNi_4Mg$ exhibits a Curie temperature $T_C = 77.6$ K which is very close to the one measured for $GdNi_2$ ($T_C = 75.0$ K; in agreement with previously published data [19–21]). The unchanged ordering temperature indicates that the sign of the coupling between Gd

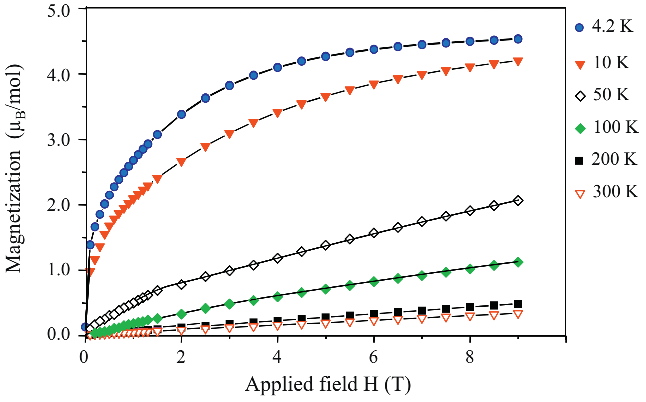

Fig. 5. $GdNi_4Mg$ magnetization as a function of applied fields at various temperatures.

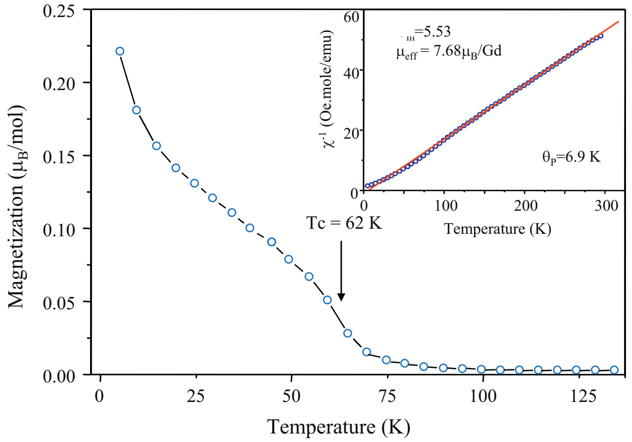

Fig. 6. $Gd_{0.75}Y_{0.25}Ni_4Mg$ magnetization as a function of temperature under an applied field of 0.3 T. Inset is the reverse susceptibility as a function of T for $GdNi_4Mg$ under 3 T.

atoms through the conduction band remains the same but that its intensity is changed.

The saturation magnetization of $GdNi_4Mg$ measured at 4.2 K under 9 T (Fig. 5) is 4.6 μ_B/mol. This is almost half the values reported for $GdNi_2$ (between 6.9 to 7.2 μ_B from [11,15,19–21]) which is in accordance with the 50% dilution of the magnetic atoms (*i.e.* $Gd_2Ni_4 \rightarrow GdNi_4Mg$).

In the RKKY model, the magnetic moment of the nickel is not taken into account. However recent studies have shown that Ni is magnetic in such alloys (0.24 μ_B estimated from the saturation magnetization at 4.2 K) and that it can couple ferrimagnetically with Gd [11,22,23]. Such a hypothesis has been done to investigate $GdNi_4Mg$ within the Molecular Field Theory [23].

The inverse of the magnetic susceptibility of $GdNi_4Mg$ under a field of 3 T is presented in the inset of Fig. 4. The curve follows a Curie Weiss law in the paramagnetic range, with a positive Curie temperature (θ_P = 25.5 K) and a paramagnetic effective magnetic moment (μ_{eff} = 7.72 μ_B/mol) close to the theoretical one of Gd^{3+}.

In order to decrease further the number of Gd atoms in the compound, two ways are offered: (i) increasing the quantity of Mg replacing Gd (*i.e.* $Gd_{1-y}Ni_4Mg_{1+y}$) or (ii) substituting the Gd atoms by a non magnetic rare earth (*i.e.* $Gd_{1-y}RE_yNi_4Mg$). We already demonstrated [2] that the solid solution $Gd_{1-y}Ni_4Mg_{1+y}$ is limited to y = 0.4 and also induces a decrease of the cell parameter due to the difference in metallic radius between Gd and Mg (*i.e.* 1.802 Å and 1.600 Å, respectively). Finally, it is rather complicated (and even almost impossible) to obtain a single phase compound. For the second way, Y atom seems the best choice as it offers the possibility of complete Gd substitution and also because the metallic radius of both Gd and Y are the same, which is not the case for La or Lu for example.

Therefore $Gd_{1-y}Y_yNi_4Mg$ compounds with y = 0.25 and 0.5 have been prepared. They exhibit almost the same lattice parameter (*i.e.* 7.036(5) and 7.029(6) Å, respectively) than the compound without Y. Their magnetic properties are presented in Figs. 6 and 7. From these two figures it can be seen that T_C decreases from 77 K to 62 K and then 45 K as the number of Gd/f.u. decreases. Nevertheless, it is also worth pointing out that the effective moment μ_{eff}/Gd determined in the paramagnetic range remains almost constant (*i.e.* close to 7.7 μ_B) so that the magnetic behaviour is still dominated by the Gd moment. As the number of Gd atoms decreases, the RKKY interactions is reduced leading to the lowering of the Curie temperature.

As it was not possible to observe the saturation in both cases, the possibility of a spin glass behaviour cannot be excluded. For that reason, AC susceptibility measurements were performed and are presented in inset in Fig. 7a for $Gd_{0.5}Y_{0.5}Ni_4Mg$. These last results confirm the existence of a ferromagnetic transition and the absence of a spin glass behaviour at low temperature. It is worth pointing out that the absence of hysteresis between the ZFC and FC curves in Fig. 7a could also allow us to suppose only a ferromagnetic transition. From inset of Fig. 7a, the inflexion point is determined to be at 48 K (close to the T_C determined from Fig. 7a). Finally, the small peak observed at 14 K (an inflexion point could also be highlighted from Fig. 7a at about 13 K) is not explained at the present time.

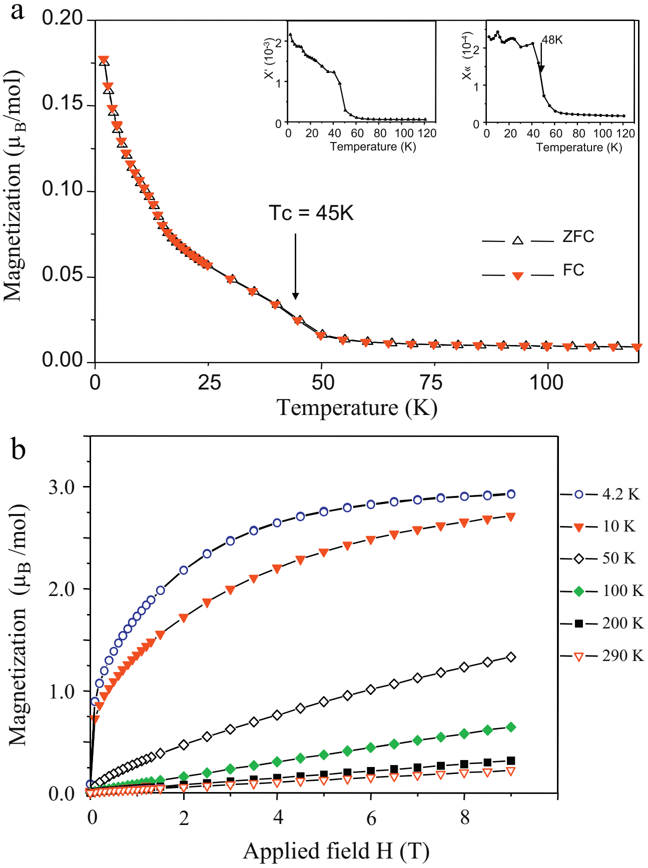

Fig. 7. (a) $Gd_{0.5}Y_{0.5}Ni_4Mg$ magnetization (ZFC and FC) as a function of temperature under an applied field of 0.1 T. Alternative susceptibility (χ' and χ") of $Gd_{0.5}Y_{0.5}Ni_4Mg$ without field and a frequency of 5000 Hz. A clear discontinuity is observed at T_C = 48 K (inflexion point). A small peak is also observed at 14 K. (b) $Gd_{0.5}Y_{0.5}Ni_4Mg$ magnetization as a function of applied field highlighting a saturation magnetization of 2.7 mB.

The saturation magnetization (Fig. 7b) is also decreasing with the number of Gd atoms in the formula (from 4.6 to 4.4 and 2.7) but not as linearly as T_C. The variation of T_C *versus* the number of Gd atoms/f.u. allows to highlight a critical number of Gd atoms/f.u. (between 1 and 0.75) below which T_C starts to decrease. Herein, the formulation of the compounds is written as follows: $Gd_{1-y}Y_yNi_4Mg$ for compounds with Mg and Gd_2Ni_4 for compound without Mg.

In order to get information about the Gd coupling through the electrons of the conduction band, $Gd_{0.5}Y_{0.5}Ni_{3.5}Al_{0.5}Mg$ was prepared and measured (a = 7.077(3) Å). In Fig. 8, the thermomagnetization under 0.3 T is presented. As previously, the effective moment determined from the Curie Weiss law (inset of Fig. 8) is close to the one of Gd^{3+}. Nevertheless, the Curie temperature drops down to 15 K, indicating that the combination of both the decrease of the conduction electron number (replacement of Ni by Al) and the increase of the cell parameter (for Al substitution, the cell

Table 2
Values of J_{ij} interaction energies deduced from the $M(T)$ curves.

Compound	J_{11} (K)	J_{12} (K)	θ_P exp (K)	Average number of nearest Gd neighbours[a]	d_{Gd-Gd} (Å)
$GdNi_2$	1.75	−3.8	70–80 [10,12,13,15]	4	3.12
$GdNi_4Mg$[b]	0.82	−3.8	25.5	12	4.98
$Gd_{0.75}Y_{0.25}Ni_4Mg$[b]	0.69	−3.8	7	9	4.98
$Gd_{0.5}Y_{0.5}Ni_4Mg$[b]	0.57	−3.8	2.5	6	4.98
$Gd_{0.5}Y_{0.5}Ni_{3.5}Al_{0.5}Mg$[b]	0.56	−3.6	5	6	5.01

[a] Coordination Gd/Gd number.

[b] The structure changes from Laves to pseudo-Laves phase.

parameter of the Al substituted solid solution follows the Vegard law with $a_{SS} = 7.04 + 0.1x$) lead to a decrease of the RKKY interaction. However, the saturation magnetization slightly increases from 2.7 to 3.1 μ_B, which can be linked with the decrease of Ni content inducing a decrease of the antiparallel coupling.

3.4. Discussion

To explain the magnetic properties it is rather convenient to use the molecular-field model with a conventional two-sublattice model for ferrimagnetism [23–26]. The experimentally obtained temperature dependence of the magnetization $M(T)$ can be fitted with three exchange interaction energies J_{ij}'s between a i and j atom as parameters. The inverse susceptibility χ^{-1} can then be calculated [26] using the J_{ij} parameters obtained from the fitting of M(T). The two sublattices considered herein are the one of Gd and the one of Ni as Mg is non magnetic. Then the sublattice molecular-fields H_{ij} can be written as follows (1 stand for Gd and 2 for Ni):

$$H_{i1} = (2Z_{11}J_{11}/g_1\mu_B)S_1 + (2Z_{12}J_{12}/g_1\mu_B)S_2$$

$$H_{i2} = (2Z_{21}J_{21}/g_2\mu_B)S_1 + (2Z_{22}J_{22}/g_2\mu_B)S_2$$

where Z_{ij} are the numbers of the j atom nearest-neighbour of an i atom, g_i is the Landé factor and S_i is the thermal average of the spin quantum numbers for the i sublattice.

The values obtained in the case of $GdNi_2$ were $J_{11} = 1.75$ K, $J_{22} = 50$ K and $J_{12} = 3.8$ K [10]. Assuming that the Ni–Ni coupling remains the same in our compounds (even when some Ni was replaced by Al), we have selected the same value for J_{22}. Moreover, Yano et al. [11] reported that the variation of J_{12} slightly affected the magnetic moment which is not the case in this study as the magnetic moment measured from the Curie Weiss law is almost constant. Therefore, for the compound without Al, only the J_{11} parameter which is the signature of the Gd–Gd interactions was refined. The results are presented in Table 2.

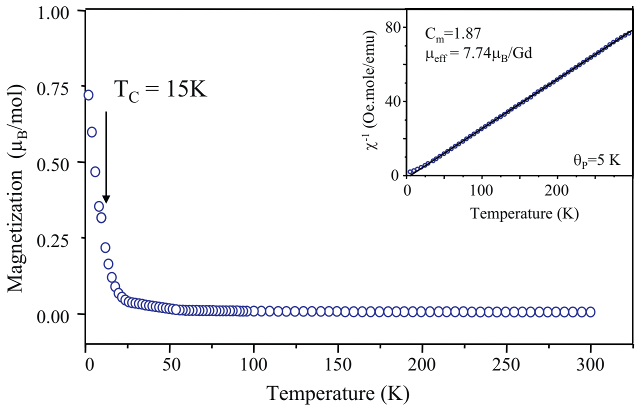

Fig. 8. $Gd_{0.5}Y_{0.5}Ni_{3.5}Al_{0.5}Mg$ magnetization as a function of temperature under an applied field of 0.3 T. Inset is the reverse susceptibility as a function of T under 3 T.

Regarding our hypothesis on J_{12} and J_{22}, the present results should not be analysed in term of absolute data but in term of relative data. Nevertheless, these results confirm all our previous interpretation regarding the intensity of the RKKY interaction. It is clear that the decrease of the number of Gd atom/f.u. leads to a severe decrease of J_{11}. Nevertheless, the J_{11} variation should be coupled with the number of closest Gd neighbour to Gd atoms and also to the distance between two Gd atoms. Going from $GdNi_2$ to $GdNi_4Mg$ leads to a decrease of the J_{11} coupling because the distance between two nearest Gd atoms is increased by 66%. The decrease of the J_{11} interaction energy is also consistent with the decrease of the θ_P value. Finally, for the compound containing aluminium, the molecular field model is less realistic as it shows a slight increase (slightly higher than the error bar) of the J_{12} interaction energy which should be coupled with a decrease of the magnetic moment (according to the model) which is not our case. Moreover, this model does not allow explaining the increase of θ_P as the J_{11} remains almost constant. Therefore, for the Al compound, the assumption of the reduction of the number of conduction electron in the 3d band should be more appropriate than the increase of Gd–Gd distances.

3.5. Effect of crystallinity on $GdNi_4Mg$ compound

Different methods for the preparation of $GdNi_4Mg$ samples have been used: melted and heat treated 10 h at 1050 °C (S1 = melted + HT), then ball-milled during 12 h (S2 = melted + HT + BM) and ball-milled during 12 h (S3 = BM), then heat treated 1 h at 600 °C (S4 = BM + HT). Such results are in rather good agreement with previous structural observations [2] but the present study goes slightly deeper. The crystallite size has been estimated using the Thomson-Cox-Hasting function in the Rietveld refinement. The crystallite size is 50(2) nm for sample S1, 30(2) nm for S2 and 10(2) nm for sample S4. The XRD pattern of sample S3 shows a rather amorphous behaviour which did not allow to calculate a crystallite size. In S2 and S4 samples, there is probably a mixture of nanocrystallized crystallites and of amorphous phase at the grain boundaries, but it has not been possible to evaluate the proportion of each in both samples.

The DSC measurements have been performed on the three S1, S2 and S4 samples: for S1, which is well crystallized, no effect is observed up to 500 °C. For S2 and S4 samples with crystallite size of 30 and 10 nm, respectively, broad peaks are observed at 390 and 360 °C, with a width of 20 and 35 °C, respectively. The energies, measured by the peak integration are at 190 kJ/g and 240 kJ/g, respectively. However, as only one heating and cooling rate has been studied, the values should be taken with care and mainly relative comparison should be done (*i.e.* absolute data should be considered with a uncertainty). These broad peaks can be attributed to the growing of the crystallite size and/or to a recrystallization of the amorphous phase. Qualitatively the temperature of the peak increases with the crystallite size. The larger width of the peak in sample S4 can be related to a larger distribution of the crystallite size.

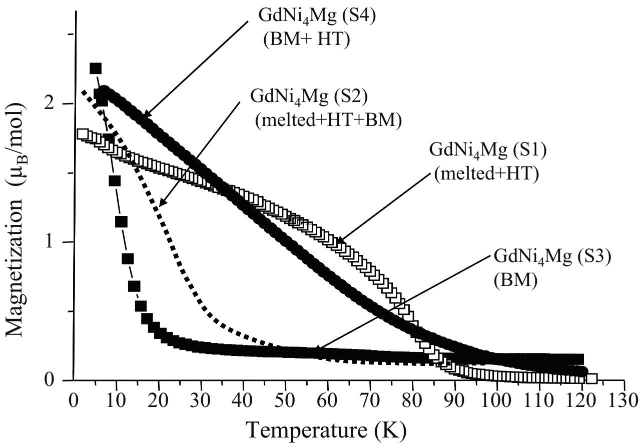

Fig. 9. Magnetization of $GdNi_4Mg$ as a function of temperature under an applied field of 0.1 T for different preparation methods, highlighting the influence of the crystallinity on the magnetic properties.

The thermomagnetization measurements at 0.1 T are presented in Fig. 9. The S1 sample displays a ferromagnetic behaviour with $T_C = 75$ K. The S2 sample displays a ferromagnetic behaviour below $T_C = 30$ K. For the S3 sample, the magnetization increases only significantly below 20 K. For the S4 sample, the magnetization increases rather monotonously below 70 K. The Curie temperature is slightly smaller than for the sample S1.

Such results are in rather good agreement with structural observations previously published [2]. The ball milled sample is almost amorphous (or nanocrystalline) and so, without long range order. The decrease and the disappearance of the ordering temperature as a function of the reduction of the crystallinity have already been reported for several compounds [27]. As an example, for $GdNi_2$ the compound prepared by melt spinning exhibits a Curie temperature of only 38 K which is significantly lower than in the crystalline compound ($T_C = 75$ K) [28]. The behaviour of the sample obtained by melting and subsequent ball milling (S2) is close to the one of the melted sample but the Curie temperature is decreased to about 30 K. These results are consistent with the fact that in amorphous or low crystallinity compound, the mean free path of the conduction electron is reduced. This result in damping of the RKKY interactions and from this point of view, a reduction of T_C is expected.

4. Conclusion

The magnetic properties of the compounds $RE_{1-y}Y_yNi_{4-x}Al_xMg$ (with $y = 0$, 0.25 and 0.5; $x = 0$, 0.5 and 1; RE = La, Ce and Gd) have been studied. The compounds with La did not exhibit any magnetic ordering but a paramagnetic behaviour. $CeNi_4Mg$ do not have a low temperature magnetic order, but a Curie Weiss behaviour with $\mu_{eff} = 2.22\ \mu_B$ has been observed. All the compounds with Gd order ferromagnetically at a temperature ranging from 77 to 15 K. The dilution of Gd atom by Y in $GdMgNi_4$ leads to a decrease of the Curie temperature below a critical number of Gd atoms (between 1 and 0.75 per formula). The effective magnetic moment is almost constant and roughly equal to 7.7 μ_B indicating a small antiparallel coupling of the Ni atoms. The lowering of the crystallinity and the replacement of Ni by Al also decrease the Curie temperature. This can be explained by a decrease of the mean free path of the conduction electron or of the number of conduction electrons leading to a decrease of the RKKY interactions between the Gd moments.

Acknowledgement

The authors are indebted to CNRS for research grants within the PIE program (PR08-2.5-3).

References

[1] L. Guénée, V. Favre-Nicolin, K. Yvon, J. Alloys Compd. 348 (1–2) (2003) 129.
[2] J-G. Roquefere, B. Chevalier, R. Pöttgen, N. Terashita, K. Asano, E. Akiba, J-L Bobet, Intermetallics 16 (2008) 179–187.
[3] B.T. Matthias, R.M. Bozorth, Phys. Rev. 109 (1958) 604.
[4] E. Burzo, A. Chelkowski, H.R. Kirchmayr, in: H.P.J. Wijn (Ed.), Landolt-Börstein, Numerical Data and Functional Relationship in Science and Technology, New Series, Magnetic Properties of Metal, vol. 19-D2, Springer, Berlin, 1990.
[5] V. Paul-Boncour, J. Alloys Compd. 367 (2004) 185–190.
[6] K.N.R. Taylor, Adv. Phys. 20 (1971) 603.
[7] W.E. Wallace, Rare Earth Intermetallics, Academic Press, New York, 1973, p. 112.
[8] H.R. Kirchmayr, C.A. Poldy, J. Magn. Magn. Mater. 8 (1978) 1.
[9] K.H.J. Buschow, in: E.P. Wohlfarth (Ed.), Ferromagnetic Materials, vol. 1, North-Holland, Amsterdam, 1980, Chapter 4.
[10] M.A. Ruderman, C. Kittel, Phys. Rev. 96 (1954) 99–102.
[11] K. Yano, I. Umehara, T. Miyazawa, Y. Adachi, K. Sato, Physica B 367 (2005) 81–85.
[12] S. Linsinger, M. Eul, C. Schwickert, R. Decourt, B. Chevalier, U.C. Rodewald, J.-L. Bobet, R. Pöttgen, Intermetallics 19 (2011) 1579.
[13] J.-L. Bobet, P. Lesportes, J.-G. Roquefere, B. Chevalier, K. Asano, K. Sakaki, E. Akiba, Int. J. Hyd. Energ. 32 (2007) 2422.
[14] R.H. Kodama, A.E. Berkowitz, E.J. Mc Niff, S. Foner, Phys. Rev. Lett. 77 (1996) 394.
[15] M. Mizumaki, K. Yano, I. Umehara, F. Ishikawa, K. Sato, A. Koizumi, N. Sakai, T. Muro, Phys. Rev. B 67 (2003) 132404.
[16] C. Geibel, U. Klinger, M. Weiden, B. Buschinger, F. Steglich, Physica B: Condens. Matter 237–238 (1997) 202.
[17] J.G. Roquefere, S.F. Matar, J. Huot, J.L. Bobet, Solid State Sci. 11 (2009) 1971.
[18] S.F. Matar, B. Chevalier, V. Eyert, J. Etourneau, Solid State Sci. 5 (10) (2003) 1385–1393.
[19] J.J. Melero, R. Burriel, M.R. Ibarra, J. Magn. Magn. Mater. 140–144 (1995) 841–842.
[20] S.K. Ma1ik, W.E. Wallace, Solid State Commun. 24 (1977) 417–419.
[21] R. Jesser, R. Clad, J. Magn. Magn. Mater. 54–57 (1986) 710–712.
[22] K. Yano, Y. Tanaka, I. Matsumoto, I. Umehara, K. Sato, H. Adachi, H. Kawata, J. Phys Condens. Matter 18 (2006) 6891–6895.
[23] P.L. Paulose, S. Patil, R. Mallik, E.V. Sampathkumaran, V. Nagarajan, Physica B 223 and 224 (1996) 382–384.
[24] K. Yano, J. Magn. Magn. Mater. 208 (2000) 207–216.
[25] J.H. Herbst, J.J. Croat, J. Appl. Phys. 53 (1982) 4304.
[26] R. Hasegawa, B.E. Argyle, L.J. Tao, AIP Conf. Proc. 24 (1975) 110.
[27] A.H. Morrish, The Physical Principles of Magnetism, Wiley Inc., New York, 1965, Chapter 9.
[28] K. Lee, N. Heiman, AIP Conf. Proc. 24 (1974) 108.